THE IMPEDANCE RESPONSE OF SEMICONDUCTORS

An Electrochemical Engineering Perspective

MARK E. ORAZEM
University of Florida
Gainesville, Florida 32611

CHEMICAL ENGINEERS working in the field of electronic materials are not normally concerned with processes taking place within the semiconductor. Most direct application of chemical engineering principle is seen in the analysis of the growth of semiconductors in the gas phase (CVD or MOCVD) or in the liquid phase (crystallization, Czochralski crystal growth, and Bridgman growth). Application of chemical engineering principles to these processes is not easy but is direct because the species of concern are not electrically charged. In contrast, the species within the semiconductor (*e.g.*, electrons, holes, ionized electron donors or acceptors) are charged, and proper analysis of processes taking place within the semiconductor requires that this electrical charge be treated.

Since ions in electrolytic solutions are also charged, the principles learned in the application of transport phenomena, reaction engineering, and thermodynamics to electrochemical systems can be applied almost directly to the study of semiconductor devices. Here, these principles are applied to interpret the impedance response of semiconducting electrodes.

BACKGROUND

Impedance techniques can be applied to semiconductors to identify the electronic structure, *i.e.*, the distribution of states within the semiconductor bandgap. A simplified schematic representation of the band structure is shown in Figure 1. Electrons can be excited from the valence or bonding orbitals to the conduction band by receiving thermal or electromagnetic (illumination) energy. The species formed by this excitation are electrons (in the conduction band) and holes (absence of an electron in the valence band). Both species are charged (electrons have a negative charge and holes have a positive charge) and can move in response to concentration or potential gradients.

The minimum energy required to excite an electron from the valence band to the conduction band is the bandgap energy. In the ideal semiconductor, electrons cannot exist at energy levels between the valence and conduction energies. In real materials, electronic states within the band gap can exist due to the presence of impurities (carbon, oxygen, and chromium are examples) or of dislocations, vacancies, or other lattice defects. These states can be electron donors or electron acceptors. Donor species are those which become positively charged when an electron is released, while acceptors become negatively charged when an electron is added. Because these species are charged, the distribution of electrical potential can be affected. Inter-band electronic states can be undesirable since they facilitate electronic transitions which can reduce the efficiency of electronic devices. In some cases, inter-band states are intentionally added when the added reaction pathways for electrons result in desired effects. Electroluminescent devices, for example, rely on emission of photons which takes place when electrons are transferred from the conduction band to an inter-band state in a large-bandgap semiconductor. The energy level of the states caused by introduction of the impurity determines the color of the emitted light. The impact of these states can be significant, even in concentrations that would seem to be very low by normal chemical engineering standards. There is, therefore, a need for developing new ways to evaluate the concentration, energy, and distribution of such electronic states.

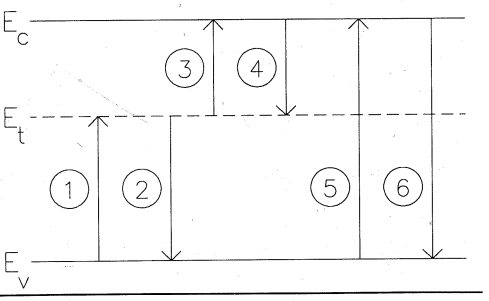

FIGURE 1. Generalized reaction scheme showing electronic transitions between the conduction band edge with energy E_c, the valence band edge with energy E_v, and a defect level with energy E_t.

A variety of techniques have been developed to study semiconductors which are based on impedance spectroscopy. We wish to focus here on a variant of electrochemical photocapacitance spectroscopy [1-5] in which the capacity of a reverse-biased electrode is measured as a function of the wavelength of incident sub-bandgap light. Let us note here that we really do not measure a capacity. Instead, we measure a periodic cell potential in response to a periodic current (or *vice-versa)* from which we calculate an impedance which has real and imaginary components. If we assume that this system behaves like an electrical circuit consisting of a capacitor and a resistor in series, we can, through regression techniques, obtain a value for a capacity and a resistance. The capacity obtained in this way is usually emphasized in this type of work since it can be easily related to the charge held in the semiconductor.

Since light of energy sufficient to cause an electronic transition will change the amount of charge held in a given

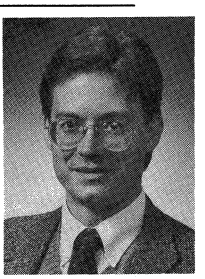

Mark Orazem is associate professor of chemical engineering at the University of Florida, where he contributes to Microfabritech (a center for study of electronic materials). He holds BS and MS degrees from Kansas State University and a PhD from UC Berkeley. His research interests include applications of impedance techniques to electrochemical systems, corrosion, and semiconductors.

state, changes in capacity at a given photon energy indicate the presence of states that allow transitions requiring that amount of energy. From this type of data we can obtain the energy levels of electronic states. The problem in this is that the largest contribution to the capacity is due to shallow level electronic states that are usually intentionally introduced as dopants. In fact, the change in capacity seen under illumination is (at best) proportional to the square root of the ratio of the defect concentration to the dopant concentration. This means that the technique of Haak and Tench [1-4] can be applied to semiconductors with a large defect concentration as compared to dopant concentration, but provides an unacceptable low signal to noise ratio when the dopant concentration is moderately large. On the other hand, the real part of the impedance, normally ignored since it is so difficult to relate to physical parameters, is very sensitive to these defects as low frequencies. We wish to focus here on the application of electrochemical principles to the problem of identifying the relationship between the real part of the impedance response and the energy, concentration, and distribution of defects. We can do this through development of a mathematical model based on the principles used in analysis of electrochemical systems. The treatment presented here follows a qualitative description of the experimental technique and the methods usually used in its analysis.

IMPEDANCE TECHNIQUES

Impedance techniques involve perturbation of a steady-state condition by a sinusoidal current or applied potential of low magnitude. A typical amplitude for an applied potential perturbation might be 10 mV, and the resulting sinusoidal current should have the same frequency, but may be shifted in phase. Thus the impedance, obtained by dividing potential by current, can be described as having real and imaginary components, *i.e.*,

$$Z = Z_r + jZ_j \quad (1)$$

A typical way to analyze impedance experiments is to compare the results to the impedance of simplified "equivalent" electrical circuits.

Equivalent Circuit Representations of Simple Systems

Electrochemists commonly present the resulting data in the form of an impedance plane plot ($-Z_j$ as a function of Z_r with frequency as a parameter). An impedance plane plot is given in Figure 2 for an electrical circuit consisting of a resistor. This is, of course, a very simple case. A Bode plot for this system (see Figure 2b) shows that the real part of the impedance is constant for all frequencies, and, since there is no phase shift, the imaginary part of the impedance is equal to zero. Thus, $Z_r = R$, and $Z_j = 0$.

The impedance data for a resistor and capacitor in series are given in Figure 3. The real part of the impedance is independent of potential, and the magnitude of the imaginary part is inversely proportional to frequency, *i.e.*, the highest values are seen at low frequencies. For this case: $Z_r = R_1$, and $Z_j = -1/\omega C_1$.

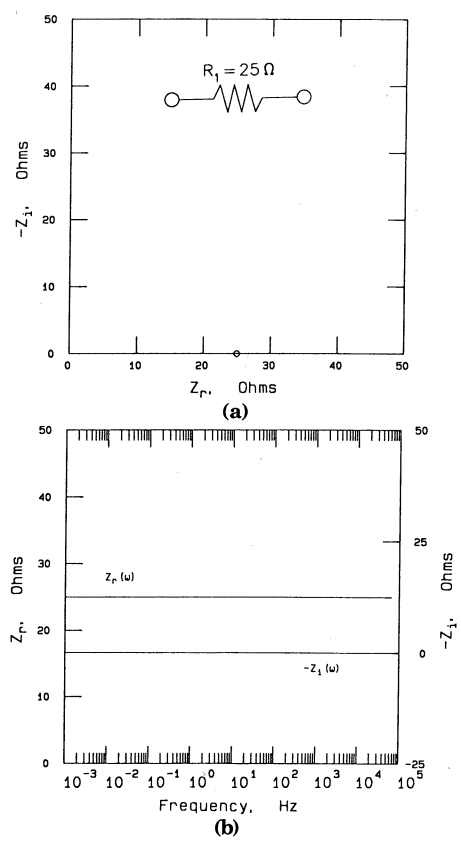

FIGURE 2. Impedance data for a system consisting of a resistor (with no capacitive component): a) impedance plane plots with frequency as a parameter; b) Bode plots for real and imaginary components of impedance.

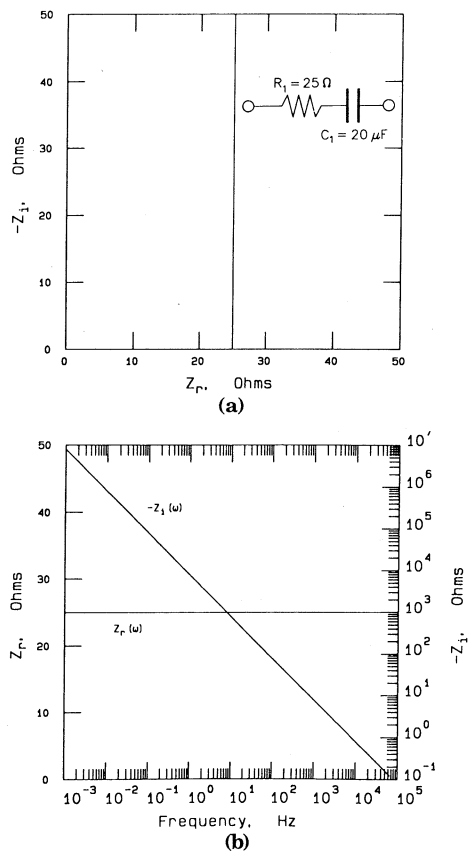

FIGURE 3. Impedance data for a system consisting of a resistor and a capacitor in series: a) impedance plane plots with frequency as a parameter; b) Bode plots for real and imaginary components of impedance.

Equivalent Circuit Representations for Electrochemical Systems

Simple electrochemical reactions at an electrode surface are often modeled in terms of the circuit shown in Figure 4. The resistance R_s is associated with the Ohmic resistance of the cell, the capacity is associated with the double layer capacity, and the resistance R_1 is related to the rate constant for the surface reaction. The impedance plane plot for this case is in the shape of a semicircle with the high frequency asymptote shifted from the origin by an amount equal to the solution resistance. Additional elements can be added to account for reactions proceeding in parallel or in series. A perfect semicircle is usually not observed experimentally, and a number of factors have been used to explain the observed depression of the semicircle. Roughening of the surface or growth of films during the course of an experiment can, in some cases, account for these observations. Mass transfer effects are also often important. These are treated by adding a Warburg element (see Figure 5). The impedance response of a Warburg element is a function of frequency and is derived by solving the convective diffusion equation for a given geometry to obtain the frequency dependent concentrations of reactants at the electrode surface. See reference 6 and chapter 9 in reference 7 for more discussion on the application of impedance techniques to typical electrochemical systems.

An Equivalent Circuit Representation for Defects in Semiconductors

The fifth case considered here is that of a second resistor and capacitor in series added in parallel to the capacitor of Figure 3. The resulting impedance data are shown in Figure 6. The magnitude of the imaginary part of the impedance is largest at lower frequencies, and the impact of the added circuit components is seen at lower frequencies. The real and imaginary components of impedance, based on the equivalent circuit given in Figure 6, are

$$Z_r = R_2 + \frac{C_1^2 R_1}{(C_1 + C_2)^2 + \omega^2 (C_1 C_2 R_1)^2} \qquad (2)$$

and

$$Z_j = -\frac{C_1 + C_2 + \omega^2 C_1^2 C_2 R_1^2}{\omega (C_1 + C_2)^2 + \omega^3 (C_1 C_2 R_1)^2} \qquad (3)$$

respectively.

If the experimental system behaves like a given electrical circuit, nonlinear regression techniques could be used to obtain values for the resistor and capacitor components in that circuit. If the electrical circuit chosen does not account for all aspects of the data, *e.g.*, if the circuit of Figure 3 is used to model the data shown in Figure 6, the circuit components will be functions of frequency. Note that the circuits given in Figures 3 and 6 do not allow passage of direct cur-

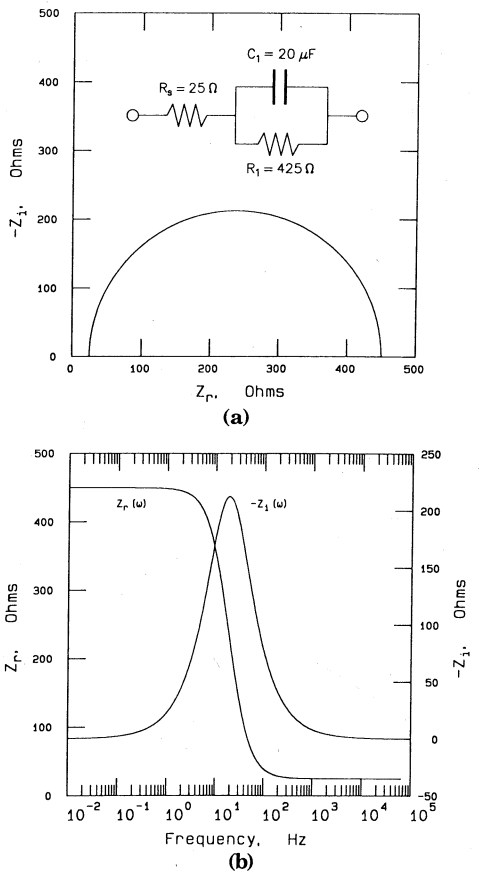

FIGURE 4. Impedance data for a system consisting of a resistor in series with the parallel combination of a capacitor and a resistor: a) impedance plane plots with frequency as a parameter; b) Bode plots for real and imaginary components of impedance.

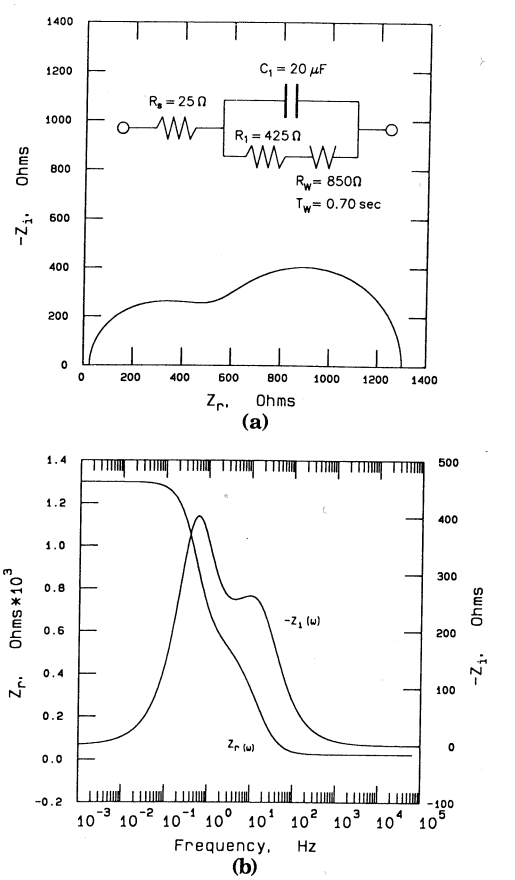

FIGURE 5. Impedance data for a system consisting of a resistor in series with the parallel combination of a capacitor and a resistor and Warburg element in series: a) impedance plane plots with frequency as a parameter; b) Bode plots for real and imaginary components of impedance.

rent. This corresponds to an ideally polarized or completely blocking electrode. To allow passage of direct current, a resistor in parallel to the other elements would be added as was done in Figures 4 and 5.

The electrical circuit given in Figure 6 is especially relevant to our system because it describes the behavior of an ideally polarized semiconductor electrode that contains a reasonable concentration of inter-band defects. In the high frequency limit,

$$Z_r = R_2 \tag{4}$$

and

$$Z_j = -\frac{1}{\omega C_2} \tag{5}$$

This behavior is more easily seen in a logarithmic impedance plane plot as shown in Figure 7. This type of plot emphasizes the high frequency data at the expense of the low frequency asymptote. The high frequency limit obscures the influence of the defects and yields the same result as would be obtained for a resistor and capacitor in series. For this reason, experimental data are frequently taken at high frequencies (greater than 10 kHz is usually sufficient). The defects, represented by C_1 and R_1, have a major influence at low frequencies, *i.e.*,

$$Z_r = R_2 + \frac{C_1^2 R_1}{(C_1 + C_2)^2} \tag{6}$$

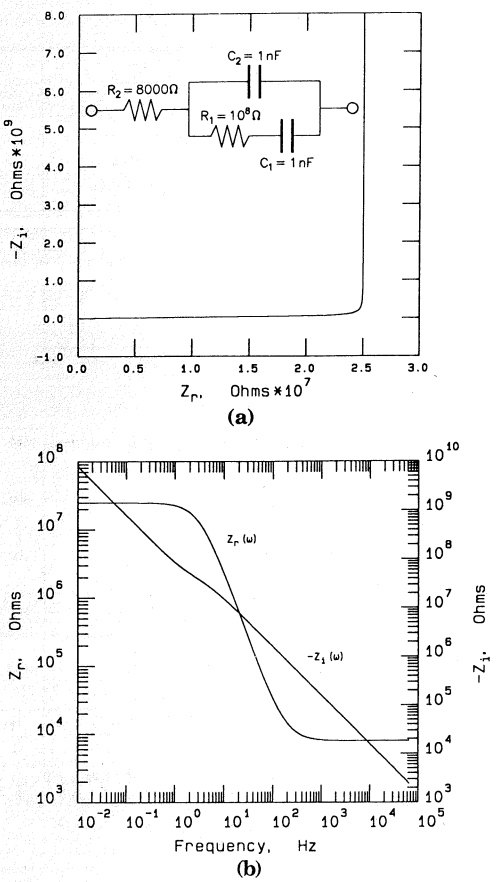

FIGURE 6. Impedance data for a system consisting of a resistor in series with the parallel combination of a capacitor and a resistor and capacitor in series: a) impedance plane plots with frequency as a parameter; b) Bode plots for real and imaginary components of impedance.

and

$$Z_j = -\frac{C_1 + C_2}{\omega(C_1 + C_2)^2} \tag{7}$$

The imaginary part of the impedance tends toward $-\infty$ while the real part of the impedance is shifted from the bulk resistance by a constant which includes the time constant associated with the defects R_1C_1 and and averaged capacity $(C_1 + C_2)^2/C_1$. This interpretation of the circuit elements is based, to a large extent, on the results of the mathematical model presented in subsequent sections.

We can compare these idealized cases to experimental results. Impedance plane plots are presented in Figure 8 with potential as a parameter for an n-GaAs electrode in contact with a mercury pool [8]. The logarithmic plot was used to emphasize the behavior at the high frequency limit. Linear regression of these data with Eqs. (2) and (3) yields frequency-independent values of circuit components which correspond to the solid line. The component values do vary with applied potential, and, if illumination had been used, the component values would vary with the photon energy of the illumination. The problem we face is how to tie these component values to physical characteristics of the semiconductor. One way to gain this intuition is to develop models for the system based on treatment of transport phenomena

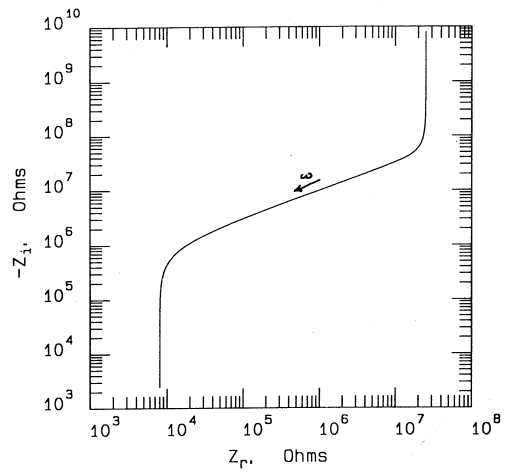

FIGURE 7. Impedance data for the system of Figure 6 consisting of a resistor in series with the parallel combination of a capacitor and a resistor and capacitor in series.

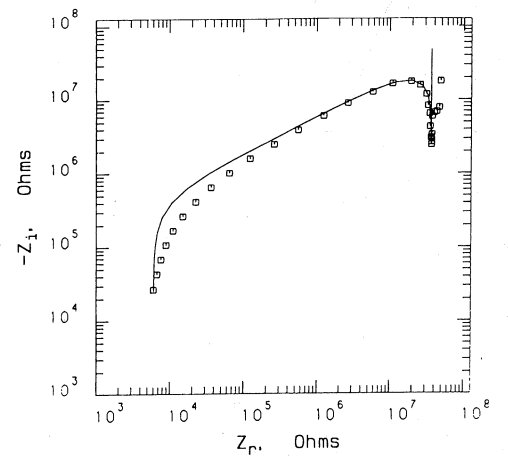

FIGURE 8. Impedance plane plot for a semi-insulating n-GaAs electrode in contact with a mercury pool [8].

and reaction kinetics and to compare the results of these models to those from the equivalent electrical circuits.

THEORETICAL DEVELOPMENT

Development of mathematical models for the impedance response of semiconducting systems generally takes place in two steps: development of a steady-state model followed by development of a model treating the sinusoidal perturbation of voltage or current about the steady-state values. Since the species of interest have a charge associated with them, we need to include treatment of electrical potential as well as concentrations. Thus, the electrostatic potential and the concentrations of electrons, holes, and ionized defect states become dependent variables for this system. The shallow-level doping species are usually assumed to be completely ionized at room temperatures and thus contribute to a fixed concentration of charge. Parts of the development presented here are given in references 9, 10, 11, and 12. References 13 and 14 provide good background to general aspects of semiconductor physics, and 15 provides a good mathematical foundation for electrochemical engineering.

Mass Transport Expressions

The electrochemical potential μ_i of a given species i can arbitrarily be separated into terms representing a secondary reference state μ_i°, a chemical contribution, and an electrical contribution, *i.e.*,

$$\mu_i = \mu_i^\circ + RT\ell n(c_i f_i) + z_i F\Phi \tag{8}$$

where c_i is the volumetric concentration of species i, f_i is the activity coefficient, z_i is the charge number, and Φ is a potential which characterizes the electrical state of the system and can be defined in many ways. This treatment is entirely analogous to the definition of chemical potentials as used for electrically neutral systems. In fact, the usual chemical potential is recovered for the case where z_i is equal to zero.

The flux N_i of species i is governed by the gradient of the electrochemical potential, given in one dimension by

$$N_i = -u_i c_i \frac{d\mu_i}{dy} \tag{9}$$

where u_i is the mobility of species i. If the semiconductor is nondegenerate, the electron and hole activity coefficients f_i can be considered to be constant, and Eq. (8) can be substituted into Eq. (9) to give the dilute solution transport expression

$$N_i = -D_i \frac{dc_i}{dy} - u_i z_i F c_i \frac{d\Phi}{dy} \tag{10}$$

where the transport properties D_i and u_i are related through the Nernst-Einstein equation; *i.e.*,

$$D_i = RTu_i \tag{11}$$

From Eq. (10), the fluxes of electrons and holes are driven by concentration and potential gradients. This distinction is a result of the separation of the chemical and electrical contributions given in Eq. (8). If desired, degenerate semiconductor conditions can be modeled by calculating the value of the activity coefficients f_i for electrons and holes (*e.g.*, [16] and [17]). The flux expression for species i is constrained by the equation of continuity, *i.e.*,

$$\frac{\partial c_i}{\partial t} = \frac{\partial N_{yi}}{\partial y} + G_i \tag{12}$$

Usually inter-band defect states are considered to be immobile; the rate of change of the concentration of ionized inter-band states is equal to their (position-dependent) rate of production, G_i.

For most electrochemical systems, the separation of charge associated with interfacial regions can be treated simply as contributing to rate constants associated with electrode kinetics. This is not appropriate for a semiconductor because this separation of charge is integral to the operation of electronic devices. Poisson's equation,

$$\frac{\partial^2\Phi}{\partial y^2} = -\frac{F}{\varepsilon_{sc}}[p - n + N_d - N_a] \tag{13}$$

can be used to relate the electrostatic potential Φ to the charge held within the semiconductor. The scaling length for this system, found by making the governing equations dimensionless, is given by the Debye length,

$$\lambda_{sc} = \left[\frac{\varepsilon_{sc} RT}{F^2(N_d - N_a)}\right]^{\frac{1}{2}} \tag{14}$$

The term $(N_d - N_a)$ includes the charge associated with partially ionized mid-bandgap acceptors (which may be a function of applied potential) as well as the completely ionized dopant species (which may have an arbitrary distribution, but is usually assumed to be independent of operating conditions).

Kinetic Expressions for Electronic Transitions

Calculation of a rate expression for G_i requires the choice of a kinetic framework. In this work, electrons are allowed to pass between the conduction band (with energy E_c), the valence band (with energy E_v), and the inter-band species (with energy E_t). A general scheme for the various electron transitions associated with this approach are shown in Figure 1. With these representations, the rates of the electronic transitions between the various energy levels can be described by applying mass action principles (*e.g.*, [13]) to give

$$r_1 = k_1 c_d^+ \tag{15}$$

$$r_2 = k_2\left(c_d^t - c_d^+\right)p \tag{16}$$

$$r_3 = k_3\left(c_d^t - c_d^+\right) \tag{17}$$

$$r_4 = k_4 c_d^+ n \tag{18}$$

$$r_5 = k_5 \tag{19}$$

and

$$r_6 = k_6 np \tag{20}$$

where k_i is the rate constant of reaction i, c_d^+ is the concentration of positively charged, inter-band donor species, c_d^t is the total concentration of inter-band donors, n is the electron concentration, and p is the hole concentration.

In the absence of inter-band states, generation of electrons and holes occurs through band-to-band mechanisms. The rate of electron generation is given by

$$G_{e^-} = k_6\left(n_i^2 - np\right) \tag{21}$$

where the two righthand terms represent thermal generation ($k_5 = k_6 n_i^2$) and recombination, respectively, and n_i is termed the "intrinsic concentration" (a physical property equal to the concentration of electrons and holes in the "ideal" undoped semiconductor). The constraint that the rates of generation and recombination are equal provides that $np = n_i^2$ under equilibrium conditions. In the presence of inter-band states, the net rate of production for electrons (and holes) is given by

$$G_{e^-} = k_6\left[1+\frac{k_2k_4p}{k_6(k_3+k_2p)}\right]\left(n_i^2 - np\right) \tag{22}$$

Again, at equilibrium, the rates of generation and recombination are equal and $np = n_i^2$.

Use of the above six kinetic expressions requires selection of the six rate constants (or three rate constants and three equilibrium constants) associated with these expressions. This apparently arbitrary selection can be approached by deriving equilibrium expressions to relate the rate constants for the reversible, homogeneous reaction pairs explicitly in terms of the energy differences between the valence band, inter-band species, and the conduction band, *i.e.*,

$$E_{12} = \frac{k_1}{k_2} = N_v g \exp\left[\frac{F(E_v - E_t)}{RT}\right] \tag{23}$$

$$E_{34} = \frac{k_3}{k_4} = \frac{N_c}{g}\exp\left[\frac{F(E_t - E_c)}{RT}\right] \tag{24}$$

and

$$E_{56} = \frac{k_5}{k_6} = N_c N_v \exp\left[\frac{F(E_v - E_c)}{RT}\right] \tag{25}$$

where E_{ij} is the equilibrium constant for reaction pair ij, g is the degeneracy associated with the inter-band state, N_c is the conduction band density of states, and N_v is the valence band density of states. These expressions were derived by assuming thermal equilibrium and substituting standard statistical expressions for electron, hole, and defect concentration in terms of energy level. The numerical value for g is determined by the electronic character of the state, *e.g.*, $g = 4$ for electron acceptors and $g = 2$ for electron donors [14].

Parameter variation studies can be further simplified by the assumption that the rate constants are interrelated such that, given energy levels for the electronic states, all rate constants can be obtained from a single rate constant. For example, the relationship,

$$k_4 = k_2\left(\frac{E_{12}}{E_{34}}\right)^{\frac{1}{2}} \tag{26}$$

was obtained by assuming that changes in the free energy of reaction associated with varying the energy of an electronic state are distributed equally between the activation energies for the forward and the reverse directions. This is similar to the standard approach used to separate the free energy of an electrochemical reaction into chemical and electrical terms. The symmetry factor in this application is assumed to have a value of 1/2 (*e.g.*, [15]).

Similar expressions can be developed for band-to-band recombination, *i.e.*,

$$k_2 = k_6\left(\frac{E_{56}}{E_{12}}\right)^{\frac{1}{2}} \tag{27}$$

The use of Eq. (27) to relate the homogeneous, band-to-band rate constant k_6 to the corresponding inter-band constants k_2 (and k_4) is equivalent to assuming that the reaction cross section is the same for recombination through trap sites as it is for direct band-to-band recombination. This assumption could easily be relaxed to account for enhanced rates of recombination through trap sites.

In the case where solar illumination is applied to the semiconductor, the expression for the optical generation of electrons under solar illumination is

$$G_{e^-,op} = q_o \gamma m \exp(-my) \tag{28}$$

where γ is the fraction of incident photons with energy greater than the bandgap E_g, m is the band-to-band absorption coefficient, and q_0 is the solar flux. Similar expressions apply for sub-bandgap illumination; however, treatment of optical excitation by light with photon energies smaller than the bandgap requires expressions for the effective absorption coefficient. Such expressions can be found in the literature (*e.g.*, [18]) for the absorption coefficient m corresponding to the transition of electrons from inter-band acceptor states to the conduction band. This absorption coefficient is a function of the inter-band state energy, the photon energy, and the concentration of ionized states. Absorption of sub-bandgap illumination is negligible for the usual values of semiconductor thickness, inter-band species density, and absorption coefficients. This allows the effects of sub-bandgap illumination to be included as a modification of the rate constants in the expressions for r_1 and r_3.

Impedance Modeling

A system whose time response y(t) to a perturbation x(t) can be described by the expression

$$b_o\frac{d^n y(t)}{dt^n} + b_1\frac{d^{n-1}y(t)}{dt^{n-1}} + \ldots + b_n y(t) = a_o\frac{d^m x(t)}{dt^m} + a_1\frac{d^{m-1}x(t)}{dt^{m-1}} + \ldots + a_m x(t) \tag{29}$$

is defined as a *linear* system. One characteristic of such a system is that a perturbation of the form $x(t) = \cos(\omega t)$ will result in a response of the form $y(t) = \cos(\omega t + \theta)$. This behavior is also observed for nonlinear systems if the amplitude of the perturbation is small enough that a first-order Taylor series expansion about the steady state is appropriate.

Experimental impedance measurements are evaluated using this theory since the current response to a sinusoidal applied potential is also sinusoidal. The important restrictions are that the system be stationary, that the system response be driven by the imposed signal, and that the imposed voltage perturbation be sufficiently small that the system can be described by Eq. (29). If these conditions are not violated, all variables of the system will take the form

$$x = \bar{x} + \left(\tilde{x}_r + j\tilde{x}_j\right)\exp(j\omega t) \tag{30}$$

where $\bar{x}$, $\tilde{x}_r$, and $\tilde{x}_j$ are functions of position, but are independent of time. This means that impedance measurements are usually made in the region where the voltage perturbation is small enough for the system to be linear, yet large enough to give a significant signal to noise ratio. For a current density given by

$$i = \bar{i} + \tilde{i}_r \exp(j\omega t) \tag{31}$$

the concentration of electrons is given by

$$n = \bar{n} + \left(\tilde{n}_r + j\tilde{n}_j\right)\exp(j\omega t) \tag{32}$$

Similar expressions are used for potential and the concentrations of holes, ionized electron acceptors, and ionized electron donors. In the above equations, an overbar represents the steady-state value, and a tilde represents the perturbation value. The actual concentration or potential at a given point in time and space is given by the real part of the expressions given above. The approach described here has

been used to model the impedance response of semiconductors in the absence of inter-band states [19, 20] and in the analysis of electrochemical systems (*e.g.*, [21-24]).

The above expressions are substituted into the governing equations which are solved sequentially for the steady-state and the sinusoidal steady-state portions, respectively. The impedance can be resolved from the calculated potential variation across the space charge region into real and imaginary components according to

$$Z_r = \frac{\Delta\tilde{\Phi}_r}{\tilde{i}_r} \tag{33}$$

and

$$Z_j = \frac{\Delta\tilde{\Phi}_j}{\tilde{i}_r} \tag{34}$$

respectively.

Steady State Boundary Conditions

The governing equations are initially solved under the steady-state condition, subject to the boundary conditions

$$\overline{N}_p = 0, \quad \frac{d\overline{\Phi}}{dy} = 0, \quad \text{and} \quad \overline{i} = 0$$

at the semiconductor-current collector interface (ohmic contact), and

$$\overline{N}_n = 0, \quad \overline{\Phi} = 0, \quad \text{and} \quad \frac{d\overline{\Phi}}{dy} = -\frac{q_{sc}}{\varepsilon_{sc}}$$

at the semiconductor-electrolyte interface (ideally polarizable contact). These conditions are appropriate for a semiconductor-mercury contact or for a semiconductor-electrolyte contact where the electrolyte is chosen so that no chemical reaction occurs.

Sinusoidal Steady State Boundary Conditions

The time-dependent equations are solved for the response to a superimposed sinusoidal current by introducing expressions for the dependent variables (such as Eq. (32)) into the governing equations and linearizing around the steady state solution obtained in the previous step. Appropriate boundary conditions for the impedance calculations are given by

$$\tilde{N}_{p,j} = \tilde{N}_{p,r} = 0, \quad \tilde{p}_j = \tilde{p}_r = 0, \quad \text{and} \quad \tilde{n}_j = \tilde{n}_r = 0$$

at the semiconductor-current-collector interface, and by

$$\tilde{N}_{n,j} = \tilde{N}_{n,r} = 0, \quad \tilde{\Phi}_j = \tilde{\Phi}_r = 0, \quad \frac{d\tilde{\Phi}_j}{dy} = \frac{\tilde{i}_r}{\varepsilon_{sc}\omega}, \quad \text{and} \quad \frac{d\tilde{\Phi}_r}{dy} = 0$$

at the semiconductor-electrolyte interface. Again, these conditions are consistent with an ideally polarized electrode where the superimposed current acts only as a charging current.

Numerical Method for Solution

The solution of the coupled differential equations is non-trivial, and a complete solution requires use of a computer. The results of this type of numerical solution are presented elsewhere [11, 12]. The point here is to emphasize that the apparently complex behavior associated with transport and reaction processes within the semiconductor in response to a sinusoidal perturbation of current or applied potential can be described by a straightforward application of principles learned in the study of electrochemical systems.

Analytic Expressions Used for Analysis of Experimental Data

Analytic solutions to the above equations have been developed that are valid in the high frequency limit. These solutions are based on integration of Poisson's equation coupled with assumption of equilibrium concentration distributions. The relationship between the applied potential and the R-C series capacitance was derived by Mott and Schottky (see, *e.g.* Joffe [25]) in the late 1930's to be (for an n-type semiconductor)

$$\frac{1}{C^2} = -\frac{2\left(V + \frac{RT}{F}\right)}{\varepsilon F(N_d - N_a)} \tag{35}$$

This is the well-known Mott-Schottky relationship.

Deviations from straight lines in Mott-Schottky plots, are frequently attributed to the influence of potential dependent charging of surface or bulk states. While deviations can also be attributed to non-uniform dopant concentrations, this interpretation is supported by analytic calculations of the contribution of defects to the space charge as a function of applied potential (*i.e.*, [26-27]).

CONCLUSIONS

The principles learned in the study of mass transport, thermodynamics, and heterogeneous and homogeneous kinetics associated with electrochemical systems can be applied directly to the transport and reaction processes that take place within a semiconductor. The theory of dilute solutions is generally appropriate, and values for needed parameters can be obtained through application of statistical thermodynamics.

ACKNOWLEDGEMENT

This material is based upon work supported by the National Science Foundation under Grant No. EET-8617057 and on work supported by DARPA under the Optoelectronics program of the Florida Initiative in Advanced Microelectronics and Materials.

NOTATION

Roman Characters

c_i	concentration of species i, cm^{-3}
C	space charge capacitance calculated from an R-C series circuit, F/cm^2
ΔC	Change in C from a chosen reference level, F/cm^2
D_i	diffusivity of species i, cm^2/s
E_a	inter-band acceptor energy, eV
E_c	conduction band energy, eV
E_d	inter-band donor energy, eV
E_f	Fermi energy, eV
E_g	bandgap energy, E_c - E_v, eV
E_{jk}	equilibrium constant for reversible reactions j and k
E_t	Energy of generalized inter-band trap species, eV
E_v	valence bandedge energy, eV
f_i	activity coefficient for generalized species i
F	Faraday's constant, 96487 C/equiv.
g	degeneracy of inter-band species
i	current density, mA
j	$\sqrt{-1}$

k_j rate constant for species j
m absorption coefficient, cm^{-1}
n electron concentration, cm^{-3}
n_i intrinsic carrier concentration, cm^{-3}
N_c effective density of conduction band states, cm^{-3}
N_d doping concentration, cm^{-3}
N_v effective density of valence band states, cm^{-3}
N_{yi} molar flux of species i, $mol/m^2 \cdot s$
r_i rate of reaction of species i, $mol/cm^{-3} \cdot s$
R universal gas constant, 8.314 J/mol•K
R resistance associated with a given electrical circuit, Ω
t time, s
T absolute temperature, K
u_i mobility of species i, $m^2/V \cdot s$
V applied potential, referenced to flatband, V
$\bar{x}$ steady state symbol for variable x
$\tilde{x}_r$ real component of the perturbation in variable x
$\tilde{x}_j$ imaginary component of the perturbation in variable x
y distance from interface, cm
z_i charge number for species, i
Z complex impedance, $\Omega \cdot cm^2$

Greek Characters

ε permittivity, Farad/cm
θ phase angle, rad
λ Debye length, cm
μ_i electrochemical potential of species i, J/mol
μ_i^o reference electrochemical potential of species i, J/mol
Φ electrostatic potential, V
$\Delta\tilde{\Phi}$ change in the real or imaginary portion of the potential across the semiconductor sample, V
ω frequency, s^{-1}

REFERENCES

1. Haak, Ron, Cameron Ogden, and Dennis Tench, "Electrochemical Photocapacitance Spectroscopy: A New Method for Characterization of Deep Levels in Semiconductors," *J. Electrochem. Soc.*, **129**, p. 891 (1982)
2. Haak, Ron, Dennis Tench, and Michael Russak, "Charge Transfer via Interface States at Polycrystalline Cadmium Selenide Electrodes," *J. Electrochem. Soc.*, **131**, p. 2709 (1984)
3. Haak, Ron, and Dennis Tench, "Electrochemical Photocapacitance Spectroscopy Method for Characterization of Deep Level and Interface States in Semiconductor Materials," *J. Electrochem. Soc.*, **131**, p. 275 (1984)
4. Haak, Ron, and Dennis Tench, "Cadmium Selenide Interface States Studied by Electrochemical Photocapacitance Spectroscopy," *J. Electrochem. Soc.*, **131**, p. 1442 (1984)
5. Allongue, P., and H. Cachet, "Photocapacitance Study of n-GaAs/Electrolyte Interfaces," *Ber. Bunsenges. Phys. Chem.*, **91**, p. 386 (1987)
6. Gabrielli, C., "Identification of Electrochemical Processes by Frequency Response Analysis," *Solartron Instruments Technical Report, Number 004/83*, p. 3 (1984)
7. Bard, Allen J., and Larry R. Faulkner, *Electrochemical Methods: Fundamentals and Applications*, John Wiley and Sons, New York (1980)
8. Smolko, Frank L., "Impedance Method for Characterization of Deep-Level States in Semiconductor Materials," MS thesis, University of Virginia, May (1988)
9. Orazem, Mark E., and John Newman, "Mathematical Modeling of Liquid-Junction Photovoltaic Cells: I. Governing Equations," *J. Electrochem. Soc.*, **131**, p. 2569 (1984a)
10. Orazem, Mark E., and John Newman, "Photoelectrochemical Devices for Solar Energy Conversion," in *Modern Aspects of Electrochemistry, Volume 18*, R.E. White, J. O'M. Bockris, and B.E. Conway, editors, Plenum Press, New York, p. 61 (1986)
11. Bonham, D. Bivings, and Mark E. Orazem, "A Mathematical Model for the A.C. Impedance of Semiconducting Electrodes," *AIChE J.*, **34**, p 465 (1988)
12. Bonham, D.B., and M.E. Orazem, "A Mathematical Model for the Influence of Deep-Level Defects on Photoelectrochemical A.C. Impedance Spectroscopy," submitted to *J. of the Electrochem. Soc.*, July 1989
13. Grove, A.S., *Physics and Technology of Semiconductor Devices*, John Wiley and Sons, New York, p. 117 (1967)
14. Sze, S.M., *Physics of Semiconductor Devices*, John Wiley and Sons, New York, p. 11 (1969)
15. Newman, John, *Electrochemical Systems*, Prentice-Hall, Inc., Englewood Cliffs, NJ, p. 173 (1973)
16. Hwang, C.J., and J.R. Brews, "Electron Activity Coefficients in Heavily Doped Semiconductors with Small Effective Mass," *J. Phys. Chem. Solids*, **32**, p. 837 (1971)
17. Bonham, D.B., and M.E. Orazem, "Activity Coefficients of Electrons and Holes in Semiconductors with a Parabolic Density of States," *J. Electrochem. Soc.*, **133**, p. 2081 (1986)
18. Moss, T.S., G.J. Burrell, and B. Ellis, *Semiconductor Optoelectronics*, John Wiley & Sons, New York, p. 60 (1973)
19. McDonald, J. Ross, "Theory of AC Space-Charge Polarization Effects in Photoconductors, Semiconductors and Electrolytes," *Phys. Rev.*, **92**, p. 4 (1953)
20. McDonald, J. Ross, "Static Space Charge and Capacitance of a Single Blocking Electrode, *J. Chem. Phys.*, **29**, p. 1346 (1958)
21. Tribollet, B., and J. Newman, "Impedance Model for a Concentrated Solution: Application to the Electrodissolution of Copper in Chloride Solutions," *J. Electrochem. Soc.*, **131**, p. 2780 (1984)
22. Cheng, C.Y., and D.-T. Chin, "Mass Transfer in AC Electrolysis: I. Theoretical Analysis Using a Film Model for Sinusoidal Current on a Rotating Hemispherical Electrode," *AIChE J.*, **30**, p. 757 (1984a)
23. Cheng, C.Y., and D.-T. Chin, "Mass Transfer in AC Electrolysis: II. Experimental Study with Sinusoidal Current," *AIChE J.*, **30**, p. 765 (1984b)
24. Cheng, C.Y., and D.-T Chin, "Mass Transfer in AC Electrolysis: III. Study of Triangular and Square-Wave Current on a Rotating Electrode," *AIChE J.*, **31**, p. 1372 (1985)
25. Joffe, J., "Schottky's Theories of Dry Solid Rectifiers," *Elec. Communication*, **22**, p. 217 (1945)
26. Dean, M.H., "The Effect of Localized Electronic States on the Interfacial Charge Distribution and Photoelectrochemical Properties of Non-Crystalline Semiconductor Electrodes," PhD dissertation, Columbia University (1988)
27. Dean, M.H., and U. Stimming, "Capacity of Semiconductor Electrodes with Multiple Bulk Electronic States: Part I. Model and Calculations for Discrete States," *J. of Electro. Chem.*, **228**, p. 135 (1987) ❐